Rok1p is a putative RNA helicase required for rRNA processing

MOLECULAR AND CELLULAR BIOLOGY, June 1997, p. 3398–3407 Vol. 17, No. 6
0270-7306/97/$04.00+0

Rok1p Is a Putative RNA Helicase Required for rRNA Processing

JAAP VENEMA,[1]* CÉCILE BOUSQUET-ANTONELLI,[2] JEAN-PAUL GELUGNE,[2] MICHÈLE CAIZERGUES-FERRER,[2] AND DAVID TOLLERVEY[1]†

European Molecular Biology Laboratory, 69117 Heidelberg, Germany,[1] and Laboratoire de Biologie Moléculaire Eucaryote du CNRS, 31062 Toulouse Cedex, France[2]

Received 21 January 1997/Returned for modification 27 February 1997/Accepted 6 March 1997

The synthesis of ribosomes involves many small nucleolar ribonucleoprotein particles (snoRNPs) as *trans*-acting factors. Yeast strains lacking the snoRNA, snR10, are viable but are impaired in growth and delayed in the early pre-rRNA cleavages at sites A_0, A_1, and A_2, which lead to the synthesis of 18S rRNA. The same cleavages are inhibited by genetic depletion of the essential snoRNP protein Gar1p. Screens for mutations showing synthetic lethality with deletion of the *SNR10* gene or with a temperature-sensitive *gar1* allele both identified the *ROK1* gene, encoding a putative, ATP-dependent RNA helicase of the DEAD-box family. The *ROK1* gene is essential for viability, and depletion of Rok1p inhibits pre-rRNA processing at sites A_0, A_1, and A_2, thereby blocking 18S rRNA synthesis. Indirect immunofluorescence by using a ProtA-Rok1p construct shows the protein to be predominantly nucleolar. These results suggest that Rok1p is required for the function of the snoRNP complex carrying out the early pre-rRNA cleavage reactions.

Ribosome biogenesis in eukaryotes takes place largely in a specialized nuclear compartment, the nucleolus (reviewed in reference 43). Here, approximately 80 ribosomal proteins associate with the four mature rRNA molecules to form the large and small ribosomal subunits. Three of the four rRNAs (18S, 5.8S, and 25–28S rRNA) are produced from a single precursor (pre-rRNA), which, in addition to the mature rRNA sequences, contains two external transcribed spacers (ETS), the 5′ ETS and 3′ ETS, and two internal transcribed spacers (ITS), ITS1 and ITS2. During maturation of the pre-rRNA, the transcribed spacers are removed in a series of processing steps carried out by endonucleases and exonucleases (see references 13 and 64 for recent reviews).

In yeast, the 35S pre-rRNA is cleaved at sites A_0, A_1, and A_2, yielding the 20S pre-rRNA, which is subsequently converted into the mature 18S rRNA (Fig. 1). A large number of *trans*-acting factors that are required for the three early cleavages have been identified. The major class comprises the small nucleolar ribonucleoprotein particles (snoRNPs), each consisting of a small RNA molecule (snoRNA) associated with a set of proteins (42). The U3, U14, and snR30 snoRNAs and the snoRNP proteins Nop1p, Sof1p, and Gar1p are all essential for cleavage at sites A_0, A_1, and A_2, while the absence of snR10 delays processing (5, 21, 28, 30, 38, 44, 59, 61). Gar1p is associated with a large subset of the snoRNAs, including snR10 and snR30, which all contain common sequence motifs, most notably an ACA sequence located 3 nucleotides from the 3′ end (4). Phenotypes observed on depletion of Gar1p and the snR30 snoRNA are very similar (21, 44), suggesting that the pre-rRNA processing defect observed on depletion of Gar1p is due mainly to inactivation of the snR30 snoRNP. Loss of snR10 gives a similar but weaker phenotype (59). The functions of U3 and U14 require direct base pairing of the RNA moiety with the pre-rRNA (5–7, 39), but the actual roles that the snoRNPs play in the cleavage reactions remain unclear. Cleavage at A_0 can be carried out in vitro by Rnt1p, the yeast homolog of RNase III, suggesting that the snoRNPs play an accessory role in A_0 cleavage rather than a catalytic one (1).

After the $A_0/A_1/A_2$ cleavages, the 3′ region of the pre-rRNA molecule, the $27SA_2$ pre-rRNA, is processed into the mature 5.8S and 25S rRNAs in a set of reactions that do not require the U3, U14, snR10, or snR30 snoRNPs. In the major processing pathway, ITS1 is cleaved at site A_3 by another snoRNP, RNase MRP (11, 40, 41, 55). This cleavage is rapidly followed by 5′ 3 3′ exonucleolytic degradation to site $B1_S$, generating the $27SB_S$ pre-rRNA (26). This processing requires Xrn1p and Rat1p (2, 26), both of which possess 5′ 3 3′ exonuclease activity in vitro (36, 37, 58). Strains lacking Xrn1p also accumulate the excised spacer fragment from the 3′ end of 18S rRNA to site A_2 in ITS1 (57) and are defective in mRNA degradation; deadenylated, decapped mRNAs are strongly stabilized in *xrn1* mutant strains (27, 46). Less direct evidence implicates Xrn1p in a range of further cellular activities (references 26, 29, and 31 and references therein).

In addition to the nucleases, another class of proteins predicted to function enzymatically in the processing and assembly of rRNA are the RNA helicases. Many members of this large, well-conserved family of proteins have an RNA-stimulated ATPase activity in vitro, while a small number have been shown to possess the ability to unwind RNA duplexes in an ATP-dependent manner (24, 49; reviewed in references 15 and 54). This activity is believed to be the common in vivo function of the members of this protein family. Putative ATP-dependent RNA helicases are found in all organisms and are implicated in all aspects of cellular RNA metabolism (15, 54). Proteins of the RNA helicase family share a number of conserved elements involved in ATP binding, substrate binding, and RNA unwinding (15, 54). The largest group of putative RNA helicases contains a common motif, DEAD, while another group, which includes several species required for pre-mRNA splicing, contains the related sequence DEAH. Two putative RNA helicases from yeast, Drs1p and Sbp4p, are required for the synthesis of 25S rRNA and/or assembly of the 60S ribo-

* Corresponding author. Present address: Department of Biochemistry & Molecular Biology, Vrije Universiteit, de Boelelaan 1083, 1081 HV Amsterdam, The Netherlands. Phone: 31 20 444 7559. Fax: 31 20 444 7553. E-mail: venema@chem.vu.nl.

† Present address: Institute of Cell and Molecular Biology, University of Edinburgh, Edinburgh EH9 3J4, United Kingdom.

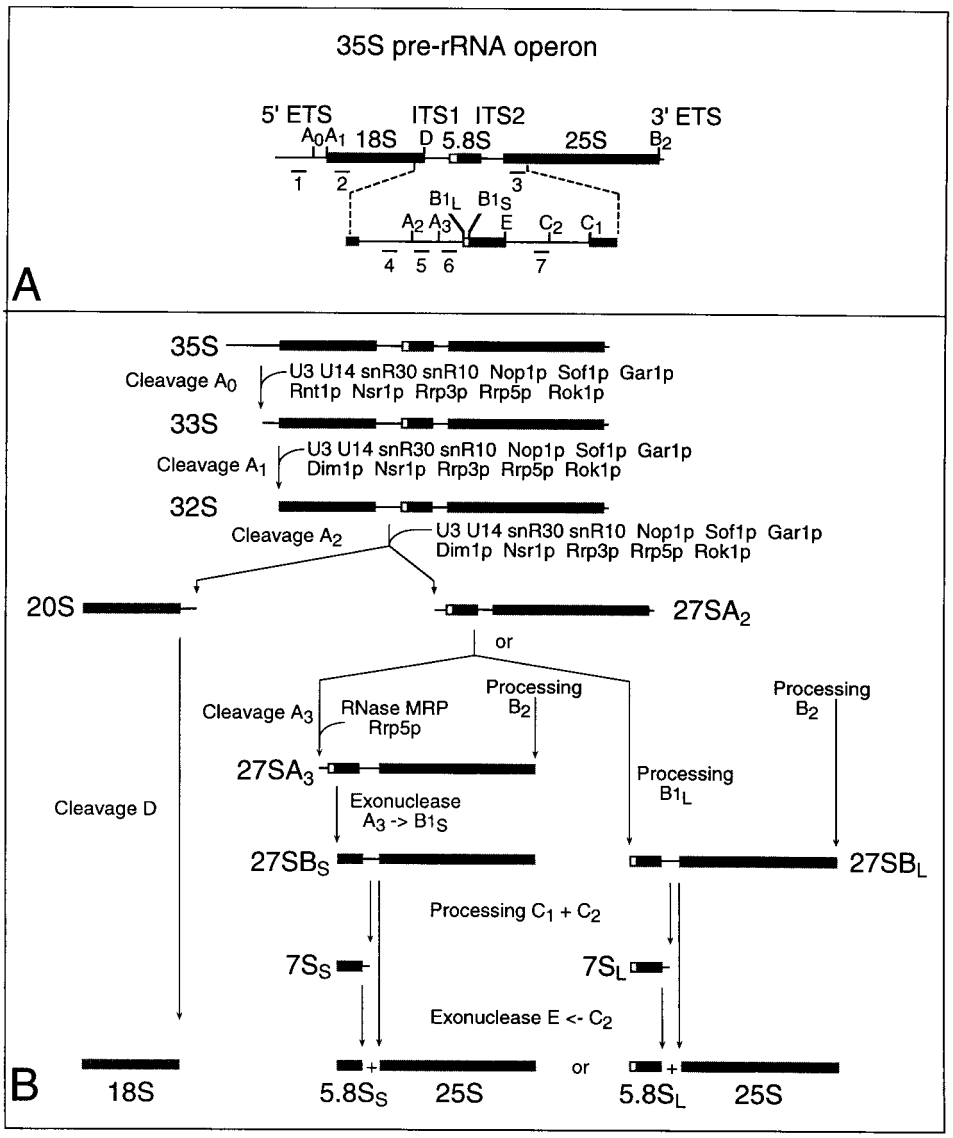

FIG. 1. Structure and processing of pre-rRNA in *S. cerevisiae*. (A) Structure of the 35S pre-rRNA. The 35S operon contains the sequences for the mature 18S, 5.8S, and 25S rRNAs separated by the two internal transcribed spacers (ITSs), ITS1 and ITS2. In addition, two external transcribed spacers (ETSs), the 5′ ETS and 3′ ETS, are present at either end. The locations of the various oligonucleotide probes (numbered from 1 to 7) used in this study are also indicated. Bars represent mature rRNA sequences, and thin lines represent transcribed spacers. (B) Pre-rRNA processing pathway. The primary transcript probably undergoes cotranscriptional processing in the 3′ ETS, generating the 35S pre-rRNA, the largest detectable precursor. The 35S pre-rRNA is rapidly cleaved at site A_0, yielding 33S pre-rRNA. This molecule is subsequently processed at sites A_1 and A_2, giving rise to the 20S and $27SA_2$ precursors. Cleavage at A_2 separates the pre-rRNAs destined for the small and large ribosomal subunits. The 20S precursor is then endonucleolytically cleaved at site D to yield the mature 18S rRNA. The $27SA_2$ precursor is processed by two alternative pathways, forming the mature 5.8S and 25S rRNAs. The major pathway involves cleavage at a second site in ITS1, A_3, rapidly followed by exonucleolytic digestion to site $B1_S$, generating the $27SB_S$ precursor. Approximately 15% of the $27SA_2$ molecules are processed at site $B1_L$, producing the $27SB_L$ pre-rRNA. At the same time as processing at B_1 is completed, the 3′ end of mature 25S rRNA is generated by processing at site B_2. The subsequent processing of both 27SB species appears to be identical. Cleavage at sites C_1 and C_2 releases the mature 25S rRNA and the 7S pre-rRNAs, which undergo rapid 3′ 3 5′ exonuclease digestion to the 3′ end of mature 5.8S rRNA (site E). *trans*-acting factors required for processing steps A_0 to A_3 are indicated (1, 64). Direct cleavage of the 35S pre-rRNA at site A_3 generates the aberrant 23S intermediate, described in the text, as well as the normal $27SA_3$ precursor.

somal subunit of which it is a component (50, 52), while another helicase, Rrp3p, is required for synthesis of the 18S rRNA (49). All three proteins belong to the DEAD-box family.

The *ROK1* gene was identified as a multicopy suppressor of a deletion of the gene encoding the exonuclease Xrn1p and found to encode a putative RNA helicase of the DEAD-box family (56). However, the function of *ROK1* was not characterized further. Here, we describe the characterization of *ROK1*, which we identified in screens for mutations showing synthetic lethality with mutations in the genes encoding Gar1p and the associated snoRNA, snR10. The absence of snR10 or the genetic depletion of Gar1p inhibits a specific set of pre-rRNA cleavage reactions leading to the synthesis of mature 18S rRNA, and Rok1p is required for the same pre-rRNA cleavages.

MATERIALS AND METHODS

Strains and plasmids. *E. coli* MH1 and DH5α were used for cloning and propagation of plasmids. Yeast strains used and constructed in this study are listed in Table 1. Construction of the plasmids pSNR10 (CEN-URA3-ADE3-

TABLE 1. Yeast strains used in this study

Strain	Genotype	Remark or reference
YJV140	*MAT***a** *ade2 his3 leu2 trp1 ura3*	65
YJV156	*MAT***a** *ade2 his3 leu2 trp1 ura3* + pRS316 (*CEN-URA3*)	YJV140 + pRS316
YJV160	*MAT***a** *ade2 ade3 his3 leu2-3,112 trp1 ura3 snr10::LEU2* + pSNR10 + pTRP1-RRP5	*snr10 sl* screen starting strain
YJV167	*MAT***a** *ade2 ade3 his3 leu2-3,112 trp1 ura3 snr10::LEU2 rok1-1* + pSNR10	*snr10 sl* strain 7
YJV172	*MAT***a** *ade2 his3 leu2 trp1 ura3 GAL::rok1* (*URA3*)	*GAL::rok1* in YJV140
YJV173	*MAT***a** *ade1-100 his4-519 leu2-3,112 ura3-52 GAL::rok1* (*URA3*)	*GAL::rok1* in D150
YJV174	*MAT***a** *ade2 his3 leu2 trp1 ura3 GAL::rok1* (*URA3*) + pTRP1-ROK1	YJV172 + pTRP1-ROK1
YJV175	*MAT***a** *ade2 his3 leu2 trp1 ura3 GAL::rok1* (*URA3*) + pTRP1-ProtA-Rok1	YJV172 + pTRP1-ProtA-Rok1
YO24	*MAT***a** *ade2-101 his3 lys2-801 trp1 ura3-52 GAL::gar1* (*URA3*)	21
YO126	*MAT*α *ade2 ade3 his3 ile leu2 lys2 trp1 tyr7 trp1-1 ura3-52 gar1::LEU2* + pJPG203 + pJPG225	$gar1^{ts}$ *sl* screen starting strain
YO88	*MAT*α *ade2 ade3 his3 ile leu2 lys2 trp1 tyr7 trp1-1 ura3-52 gar1::LEU2 rok1-2* + pJPG203 + pJPG225	$gar1^{ts}$ *sl* strain slc 94

SNR10), pHIS3-SNR10 (CEN-HIS3-SNR10) and pTRP1-RRP5 (CEN-TRP1-RRP5) is described in reference 65. Construction of the vectors pJPG53 (CEN-TRP1-GAR1 flanking regions) and pJPG67 (CEN-TRP1-GAR1) is described in reference 20. pJPG53 contains a *Bam*HI site separating the *GAR1* upstream and downstream regions, which can be used for insertion of *GAR1* wild-type or mutant alleles. Vector pJPG219 (CEN–TRP1–gar1-10) was produced in this way by insertion of the *Bam*HI cassette containing the *gar1-10* mutant allele (see below). Vector pJPG203 (CEN-ADE3-URA3-GAR1) was constructed by insertion of a 1.6-kb *Sal*I-*Pvu*II fragment from pJPG67, containing the *GAR1* gene, into the *Sal*I-*Nru*I sites of pCH1122 (33). To obtain pJPG208 (CEN-LYS2-GAR1), a blunt-ended *Sal*I-*Sma*I fragment from YDpK (8), containing the *LYS2* gene, was isolated and used to replace the *Bgl*II fragment containing the *URA3* marker gene in pFL38 (accession no. X70482). This plasmid was then used for the insertion of an *Eco*RI-*Sal*I fragment from pJPG67, containing the *GAR1* gene, yielding pJPG208. To confer erythromycin resistance, a *Bst*UI fragment containing the *ermA* gene was inserted into the *Sca*I site of pJPG208, yielding pJPG223 (CEN-LYS2-ermA-GAR1). In this vector, the wild-type *GAR1* gene was substituted by the *Bam*HI cassette from pJPG219, containing the *gar1-10* mutant allele, to obtain pJPG225 (CEN–LYS2–ermA–gar1-10).

Isolation of *gar1* conditional alleles. To isolate *gar1* thermosensitive alleles, a *Bam*HI cassette containing *GAR1* was cloned into the *Bam*HI site of pBS(KS+). Random mutations were generated by PCR with low dATP and dGTP concentrations (10). From the PCR product, a 627-bp *Bam*HI fragment, containing *GAR1*, was cloned into the *Bam*HI site of pJPG53 (CEN-TRP1-GAR1 flanking regions) and transformed to *E. coli*. Of the approximately 60,000 transformants, 90% were found to bear the *GAR1* insert. Plasmid DNA was extracted and used to transform yeast strain YO24 (*GAL::gar1* [Table 1]). Yeast transformants were selected on YPD plates at 25°C and then replica plated onto YPD at two different temperatures, 37 and 15°C, to identify temperature-sensitive (*ts*) and cold-sensitive (*cs*) mutants, respectively. Among 16,000 yeast transformants, we obtained 3 *ts* and 4 *cs* strains. The mutant alleles were recovered and sequenced. One *ts* allele (*gar1-10*), which codes for a Gar1p mutant protein truncated at position 158 and bearing three point mutations (G12V, V52G, and F89I), was selected for this study, and the plasmid containing the *gar1-10* allele was designated pJPG219.

Isolation of *sl* mutants. Strain YJV160 carries the *ade2*, *ade3*, and *snr10::LEU2* alleles and harbors a wild-type *SNR10* gene on an *ADE3/URA3*-containing plasmid (pSNR10 [Table 1]). To avoid the reisolation of *rrp5* mutations, identified in a previous synthetic-lethal (*sl*) screen with *snr10* (65), YJV160 also carries the *RRP5* gene on a plasmid (pTRP1-RRP5). YJV160 was grown in SD-Leu-Trp-Ura until mid-exponential phase and plated onto 4% YPD plates (YPD plates containing 4% [wt/vol] glucose). The plates were then UV irradiated with a dose resulting in approximately 15% survival and incubated for 6 days at 30°C. Strain YO126 carries the *ade2*, *ade3*, and *gar1::LEU2* alleles and harbors a wild-type *GAR1* gene on an *ADE3/URA3*-containing plasmid (pJPG203) and the temperature-sensitive *gar1-10* allele on a *LYS2*-containing vector (pJPG225). Strain YO126 was grown in SD-Leu-Lys-Ura medium until mid-exponential phase, washed in 0.9% NaCl, and resuspended in 0.9% NaCl at a density of 10^8 cells/ml. A 4-ml volume of this cell suspension was transferred to a petri dish (diameter, 55 mm) and exposed to UV for 30 s with agitation (yielding 10 to 15% survival). The suspension was divided into 0.5-ml aliquots, and, after addition of 1.5 ml of SD-Leu-Lys-Ura medium, grown for 4 h at 25°C in the dark. The cells were then plated on SD-Leu-Lys plates and incubated for 4 days at 25°C. Colonies were replica plated onto 4% YPD plates and incubated for 4 days at 25°C, and then red colonies were restreaked onto 4% YPD plates. In both screens, from a total number of approximately 20,000 colonies, 6 nonsectoring, red strains were identified after restreaking twice onto fresh 4% YPD plates. They were all streaked on plates containing 5-fluoroorotic acid (5-FOA) and incubated for 7 days. Three strains identified in the *snr10 sl* screen were unable to grow on 5-FOA medium and were then transformed with pHIS3-SNR10 or with a control vector, pRS313 (19). In two strains (*sl* 7 and *sl* 126) sectoring was restored upon transformation with pHIS3-SNR10 but not with pRS313, showing that they carried mutations which are *sl* with the *SNR10* gene disruption. Similarly, three *gar1-10 sl* strains that were unable to grow on 5-FOA (slc 16, slc 94, and slc 251) were transformed with pJPG67 (CEN-TRP1-GAR1) or pJPG219 (CEN–TRP1–gar1-10). In all cases, the sectoring phenotype was restored with the wild-type *GAR1* gene but not with the *gar1-10* allele, showing that the nonsectoring phenotype is due to colethality with the *gar1* mutant allele. One of the *sl* strains, slc 94, was crossed to YO126MAT**a**, and the resulting diploid was sporulated. Upon tetrad dissection, we observed a 2::2 segregation of the *sl* phenotype, indicating that it was caused by a mutation in a single gene.

Cloning of *ROK1*. Strains *sl* 7 (YJV167 [Table 1]) and slc 94 (YO88 [Table 1]) were transformed with a yeast genomic library by the lithium acetate method (18) and the transformants were replica plated onto 4% YPD plates to identify sectoring colonies. In both screens, the library plasmid was recovered from 12 sectoring strains. Nine plasmids recovered from YJV167 transformants carried the wild-type *SNR10* gene, whereas the other three carried different overlapping fragments. Of the plasmids recovered from YO88, 10 contained either the wild-type *GAR1* or *ADE2* gene whereas the other 2 contained an undetermined genomic fragment. Upon determination of the sequence of the terminal regions, all library inserts contained a region from chromosome VII. The fragment common to the three YJV167 plasmids contained three complete open reading frames (ORFs); two ORFs corresponded to known genes, *NSP49* and *ROK1*, whereas the third ORF (gene G1654) was still uncharacterized. These plasmids were transformed back to strain YJV167 and found to complement the sectoring phenotype. Three internal deletions were then constructed in one of the library plasmids, p55a, disrupting each of the individual ORFs, and transformed to strain YJV167. The plasmids with deletions in either the *NSP49* gene or the unknown ORF were still able to complement the sectoring phenotype of *sl* strain YJV167, whereas that with *ROK1* deleted was not. One of the library plasmids identified in the *gar1-10* screen contained four ORFs, three corresponding to already known genes, *ROK1*, *SUA5*, and *PMR1*, and one corresponding to an unknown gene (G1654). The library plasmid was transformed back to strain YO88 and found to complement the synthetic-lethal phenotype. A *Sgr*AI-*Ecl*136 fragment containing the *ROK1* gene was then subcloned into pFL39 and was shown to be able to complement the *sl* phenotype of strain YO88.

Strains slc 94 (YO88) and slc 94+pTRP1-ROK1 were cured of plasmid pJPG225 (CEN-LYS2-ermA-gar1-10) and grown in SD-Leu and SD-Leu-Trp medium, respectively, until mid-exponential phase. Drops containing 20,000, 10,000, 5,000, 1,000, 200, and 40 cells, respectively, were spotted on YPD plates and incubated at 13, 17, 25, and 37°C. Strain slc 94, carrying the *rok1 sl* allele, exhibited a growth defect at 13 and 17°C in comparison to strain slc 94 complemented by the plasmid-borne, wild-type *ROK1* gene, whereas cells grew normally at 25 and 37°C. The *ROK1* sequence is available under accession no. Z34901.

Cloning and sequencing of the *rok1 sl* alleles. The *rok1-1* allele from strain YJV167 was cloned by gap repair (51). For this, the library plasmid p55a was digested with *Nco*I and *Hpa*I, which introduces a 4.5-kb deletion encompassing the *ROK1* locus. The linearized plasmid was gel purified and retransformed to strains YJV167 and YJV160, after which His^+ transformants were selected. For each strain, the plasmid from four independent transformants was rescued by transformation of a yeast miniprep to *E. coli*. The intact plasmids were retransformed to strain YJV167, and in all cases, the constructs derived from strain YJV160 complemented the *sl* phenotype whereas those derived from YJV167 did not. To clone the mutant *rok1-2* allele from *sl* strain YO88, we prepared genomic DNA from this strain as well as the parental YO126 strain. Genomic DNA (50 μg) was digested with *Eco*RI-*Hin*dIII and separated on a 1.2% preparative agarose gel. DNA ranging in size from 2.5 to 3.5 kb (the *Eco*RI-*Hin*dIII fragment containing *ROK1* is 3 kb) was gel purified and cloned into pBS(KS+). The resulting partial genomic library was transformed into DH5α, and approximately 2,000 transformants were screened by colony hybridization (53) with a 40-mer oligonucleotide probe complementary to *ROK1*. The sequences from the parental *ROK1* genes and the two *rok1* mutant alleles were determined by

dideoxy sequencing. For this, a 1.7-kb *Nco*I-*Tth111*I fragment from representative clones, containing the *ROK1* gene, was subcloned into pBS(KS+) and entirely sequenced.

Construction of the *GAL::rok1* allele. A 2.7-kb *Eco*RI-*Sac*I fragment containing the *ROK1* gene was subcloned from the library plasmid p55a into pBS(KS+), yielding pBS-ROK1. This plasmid was linearized with *Nco*I, present at the ATG start codon of the *ROK1* gene, blunt ended with Klenow DNA polymerase, and used for insertion of a 1.5-kb blunt-ended *Hin*dIII-*Bam*HI fragment from plasmid pLGSD5, containing the *URA3* gene and the *GAL10* promoter (23). The resulting plasmid, pBS-GAL::rok1, contains the *ROK1* gene fused to the *GAL10* promoter at the *Bam*HI and *Nco*I sites. From pBS-GAL::rok1, a linear 4.2-kb *Eco*RI-*Sac*I fragment, containing the *GAL::rok1* gene and 550 bp of both 5′- and 3′-flanking sequences, was gel purified and used to transform strain YJV140 (Table 1). Colonies were initially selected on SGal-Ura plates and restreaked on YPD and YPGal plates to check for galactose dependence. Six galactose-dependent strains were analyzed by Southern hybridization to confirm correct integration. One such strain was chosen and designated YJV172 (Table 1). The *GAL::rok1* allele was also integrated into another wild-type host strain, D150, yielding strain YJV173 (Table 1).

In vivo depletion of Rok1p. Strain YJV172 (*GAL::rok1*) was grown in liquid SGal-Ura medium until mid-exponential phase. Cells were harvested by centrifugation and resuspended to an optical density at 600 nm (OD_{600}) of 0.06 in SD-Ura. Cell growth was monitored over a period of up to 50 h, during which the cultures were regularly diluted with prewarmed medium to maintain exponential growth. As a control, YJV140 transformed with pRS316 (strain YJV156) was used. For RNA isolation, cells were harvested at 0, 12, 24, 36, and 48 h after the shift to glucose-based medium.

RNA analysis. RNA isolation, Northern hybridization, and primer extension were all carried out as described previously (6, 59, 65). In all experiments, RNA samples corresponding to 0.2 OD_{600} unit of cells were used, except for primer extension from within the mature rRNA regions. In this case, RNA corresponding to 0.02 OD_{600} unit of cells was used, whereas the ^{32}P-labelled primer was mixed with a 10-fold molar excess of unlabelled primer. The following oligonucleotides were used for Northern hybridization and primer extension (see Fig. 1): 5′-TCGGGTCTCTCTGCTGC-3′, 5′-CATGGCTTAATCTTTGAGAC-3′, 5′-CTCCGCTTATTGATATGC-3′, 5′-GCTCTTTGCTCTTGCC-3′, 5′-TGTTACCTCTGGGCCC-3′, 5′-CCAGTTACGAAAATTCTTG-3′, and 5′-GGCCAGCAATTTCAAGTTA-3′.

Construction of the *ProtA::rok1* allele. Plasmid pTRP1-ROK1 contains a 2.7-kb *Eco*RI-*Sac*I fragment from library plasmid p55a cloned into pRS314 (CEN-TRP1). A 400-bp *Nco*I fragment, encoding two immunoglobulin G (IgG)-binding domains of *Staphylococcus aureus* protein A, was then cloned into the naturally occurring *Nco*I site at the ATG start codon of the *ROK1* gene, yielding plasmid pTRP1-ProtA::rok1. Plasmids pTRP1-ROK1 and pTRP1-ProtA::rok1 were transformed to strain YJV172 (*GAL::rok1*) and selected on SGal-Trp-Ura plates. Transformants were streaked on YPD to test the functionality of the plasmid-borne *ROK1* (strain YJV174) and *ProtA::rok1* (YJV175) genes, respectively (Table 1).

Immunofluorescence. YJV174 and YJV175 cells were grown in YPD to mid-exponential phase, fixed by incubation in 4% (vol/vol) formaldehyde for 1 h at room temperature, and spheroplasted. Immunofluorescence was then performed by standard procedures (9, 22). Nop1p was detected with mouse monoclonal antibody MAb66 (3) (kindly provided by J. P. Aris, University of Florida, Gainesville, Fla.) and a secondary goat anti-mouse antibody coupled to Texas Red (Jackson Immunoresearch, West Grove, Pa.), both at a 1:200 dilution. ProtA-Rok1p was detected with a rabbit anti-protein A antibody at 1:200 followed by a secondary goat anti-rabbit antibody coupled to fluorescein isothiocyanate (FITC) at 1:160 (both from Sigma). To stain nuclear DNA, 4′,6-diamidino-2-phenylindole (DAPI) was included in the final wash step at 1 μg/ml.

RESULTS

Identification of *ROK1* in synthetic-lethal screens. The screens for *sl* mutations were based on the *ade2/ade3* red/white colony sectoring assay (32, 33, 65) (see Materials and Methods for details of the screens). Two starting strains were used. Strain YJV160 carries an insertional disruption of the chromosomal *SNR10* gene and the wild-type *SNR10* gene on an *ADE3URA3* plasmid (pSNR10). Strain YO126 carries a chromosomal disruption of the *GAR1* gene, the wild-type *GAR1* gene on an *ADE3 URA3* plasmid (pJPG203), and a *ts gar1-10* allele on a *LYS2* plasmid (pJPG225). The growth of strains lacking *SNR10* or carrying the *gar1-10* allele is only mildly impaired, and on nonselective YPD plates the plasmids containing the wild-type *SNR10* or *GAR1* genes can be lost, yielding red/white-sectoring colonies. After mutagenesis by UV irradiation, surviving colonies were screened microscopically for nonsectoring mutants. These strains were streaked on plates containing 5-FOA. *sl* mutants are not able to lose the wild-type *SNR10* or *GAR1* plasmids and should be unable to grow on media containing 5-FOA because of the presence of the *URA3* gene on the plasmid. Two such strains were identified in the screen with *snr10*; both strains regained sectoring when transformed with an *SNR10* gene but not with an empty vector, demonstrating that these cells carried *sl* with the *snr10* deletion. By the same criteria, three *sl* strains were identified in the screen with *gar1-10*.

The gene responsible for the synthetic lethality with *snr10* in strain YJV167 (*sl* 7) was cloned by complementation of the sectoring phenotype. A yeast genomic library was transformed to YJV167, and the library plasmid was recovered from 12 resectoring colonies. In nine cases, the wild-type *SNR10* gene was cloned, while the three remaining plasmids contained overlapping fragments derived from a region of chromosome VII. The fragment common to the inserts contained three complete ORFs; two corresponded to known genes, *NSP49* and *ROK1*, whereas the third ORF (G1654) was uncharacterized. Internal deletions were made in each of the ORFs and tested for complementation. Only the deletion in *ROK1* abolished complementation of the sectoring phenotype. The *rok1-1* allele in *sl* strain YJV167 and the *ROK1* gene from the parental YJV160 strain were cloned by gap repair and retransformation into *E. coli* (see Materials and Methods). When intact plasmids carrying the parental *ROK1* gene were reintroduced in the *sl* strain YJV167, red/white sectoring was restored, whereas this was not the case for plasmids carrying the *rok1-1* allele derived from YJV167. These results demonstrate that the mutation responsible for the synthetic lethality with *snr10* lies within the *ROK1* gene.

One of the strains identified in the *sl* screen with *gar1-10*, slc 94 (YO88 [Table 1]), was crossed with the parental strain, the diploid strain was sporulated, and tetrads were dissected. For each tetrad, haploid spores were transformed with plasmid pJPG219 (CEN–TRP1–gar1-10) and transformants were tested for growth on 5-FOA, colony sectoring, and thermosensitive growth. In all cases, two sectoring haploids that grew normally on 5-FOA and two nonsectoring haploids unable to grow on 5-FOA were obtained. This 2:2 segregation shows that a mutation in a single gene is responsible for the *sl* phenotype. Moreover, all nonsectoring haploid strains exhibited a cold-sensitive growth phenotype, indicating that the *sl* mutation induced in strain slc 94 confers a cold-sensitive growth phenotype. To clone the wild-type allele of this gene, strain YO88 was transformed with a genomic library and 12 sectoring colonies were selected. Among these, 10 transformants carried either the wild-type *GAR1* gene or the *ADE2* gene. The plasmids from the two remaining transformants were recovered and, upon retransformation into the slc 94 strain, shown to complement the *sl* phenotype. One of the plasmids was partially sequenced and shown to contain a fragment from chromosome VII comprising the *ROK1* gene, as well as the *SUA5* and *PMR1* genes and an uncharacterized ORF (G1654). Subcloning showed that the *ROK1* gene alone was able to restore both sectoring and growth at 13°C of the slc 94 strain. The *ROK1* genes were recovered from the parental strain, YO88, and from the *sl* strain, YO126 (Table 1), by screening partial genomic libraries. Upon retransformation of both alleles to strain slc 94, the *ROK1* gene recovered from the wild-type strain restored red/white sectoring and growth on 5-FOA-containing medium, whereas this was not the case for the *rok1-2* allele recovered from the *sl* strain. A mutation in *ROK1* is therefore also *sl* with the *gar1-10* allele. Interestingly, the *rok1-2* allele is also *sl* with *snr10*, as shown by the inability to

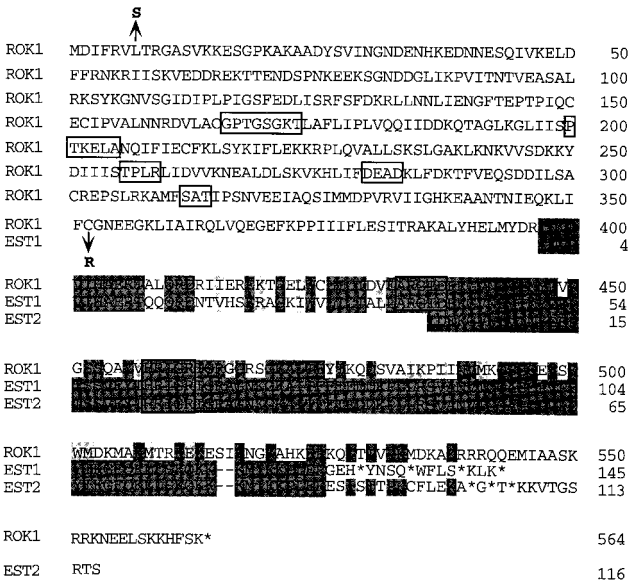

FIG. 2. Alignment of Rok1p with its putative human homologs. The predicted amino acid sequence of the Rok1p protein (ROK1) and alignment of the C-terminal region with two overlapping human ESTs (EST1 and EST2; accession no. N30525 and N30537, respectively) are shown. Stop codons are represented by asterisks. Identities are indicated by dark shading, and similarities are indicated by light shading. Both ESTs probably contain frameshifts in their C-terminal region, as a result of which the alignment fails after residue 126 (EST1) or 101 (EST2). Motifs which are conserved among (putative) RNA helicases are boxed (54). The mutations identified in the *rok1-1* (Leu^7 3 Ser) and *rok1-2* (Cys^{352} 3 Arg) *sl* alleles are also indicated.

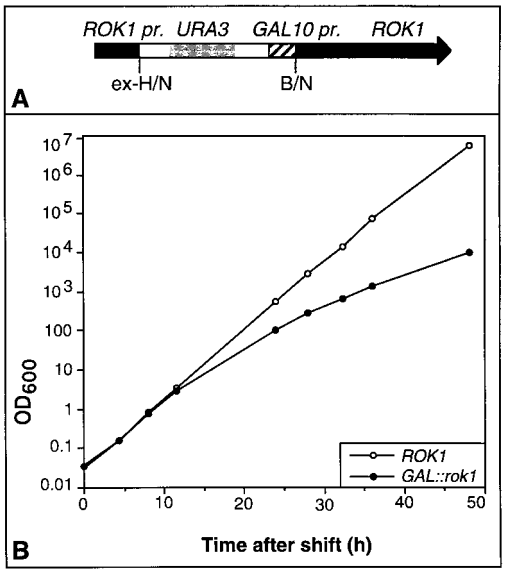

FIG. 3. Construction and growth of the *GAL::rok1* strain. (A) Schematic representation of the *GAL::rok1* allele. A *Hin*dIII (H)-*Bam*HI (B) fragment from pLGSD5, carrying the *URA3* gene and the *GAL1/10* promoter cassette (23), was inserted into the *Nco*I (N) site, present at the ATG of the *ROK1* gene. This construct was transformed as a linear fragment to haploid strain YJV140 (Table 1) and integrated into the *ROK1* locus. Galactose-dependent transformants were verified by Southern analysis (data not shown). (B) Growth of the *GAL::rok1* strain YJV172 (solid symbols) and its wild-type isogenic counterpart YJV156 (open symbols) after transfer from galactose- to glucose-based medium at $t = 0$ h. The cell density was measured at regular intervals, and the cultures were periodically diluted to maintain exponential growth.

complement the nonsectoring phenotype of the *sl* strain YJV167.

ROK1 is predicted to encode a DEAD-box, ATP-dependent RNA helicase of 564 amino acids (64 kDa). The protein is basic (pI = 9.2) and contains a high percentage of hydrophilic amino acids. In addition to all of the conserved helicase motifs present in the central domain, Rok1p contains N- and C-terminal domains of approximately 160 and 80 residues, respectively. These regions, which are distinct from those in other RNA helicases, are presumed to confer unique functions to the different DEAD-box proteins. The *rok1 sl* alleles were cloned into pBS(KS+) and entirely sequenced. The *rok1-1* mutation, *sl* with *snr10*, consists of a single T 3 C transition at position +20 that results in a Leu^7 3 Ser amino acid substitution near the N terminus of the protein (Fig. 2). The *rok1-2* mutation is also a T 3 C transition at position +1054, thereby altering Cys^{352} to Arg (Fig. 2). Neither mutation is in the proximity of any of the conserved RNA helicase motifs. However, the cold-sensitive growth phenotype associated with *rok1-2* may be due to the lack of a cysteine residue, which might affect the folding of the Rok1p protein. Rok1p contains a total of nine Cys residues and therefore has the potential to form four internal disulfide bridges.

A search in the database resulted in the identification of two overlapping expressed sequence tags (ESTs) from humans, which show homology to a region in the C-terminal part of Rok1p. Part of the homology resides in the central helicase domain, but the conservation extends into the unique, C-terminal domain (Fig. 2). The *ROK1* gene had previously been cloned as a multicopy suppressor of a deletion of the *XRN1/KEM1* gene and was shown to be essential for cell viability (56). The fact that the *ROK1* gene functionally interacts with *GAR1*, *SNR10*, and *XRN1*, all of which are involved in pre-rRNA processing, suggested that Rok1p might also function in this activity.

Genetic depletion of Rok1p inhibits the synthesis of 18S rRNA. Since *ROK1* had been shown to be essential for cell viability (56), we analyzed the effect of depletion of the Rok1p protein by using a conditional-lethal mutant. The *ROK1* gene was placed under control of the *GAL1* promoter inserted at the *Nco*I site, which occurs naturally at the ATG start codon (Fig. 3) (see Materials and Methods). The *GAL::rok1* gene was integrated at the *ROK1* genomic locus by transformation into the wild-type haploid strain YJV140 followed by screening for galactose dependence. In phenotypically correct, GAL^d strains, the correct integration of the *GAL::rok1* allele was confirmed by Southern analysis (data not shown). One strain, YJV172, was used for subsequent experiments (Table 1).

The growth rates of the *GAL::rok1* strain and an otherwise isogenic wild-type strain, YJV156 (Table 1), were indistinguishable on galactose medium. Following transfer to glucose medium, both strains had an initial doubling time of approximately 1.7 h. The wild-type control strain maintained this growth rate, while growth of the *GAL::rok1* strain slowed approximately 12 h after transfer, consistent with the gradual depletion of an essential cellular component (Fig. 3).

To analyze the effect of Rok1p depletion on rRNA synthesis, total RNA was isolated from the *GAL::rok1* and *ROK1* strains at various time points after the shift to glucose and analyzed by Northern hybridization (Fig. 4). Hybridization with oligonucleotides complementary to the mature rRNAs shows that depletion of Rok1p does not affect the level of 25S rRNA (Fig. 4A). The level of 18S rRNA remains constant until 12 h after transfer to glucose, consistent with the absence of any growth defect up to that time. At later time points, the level of 18S rRNA is

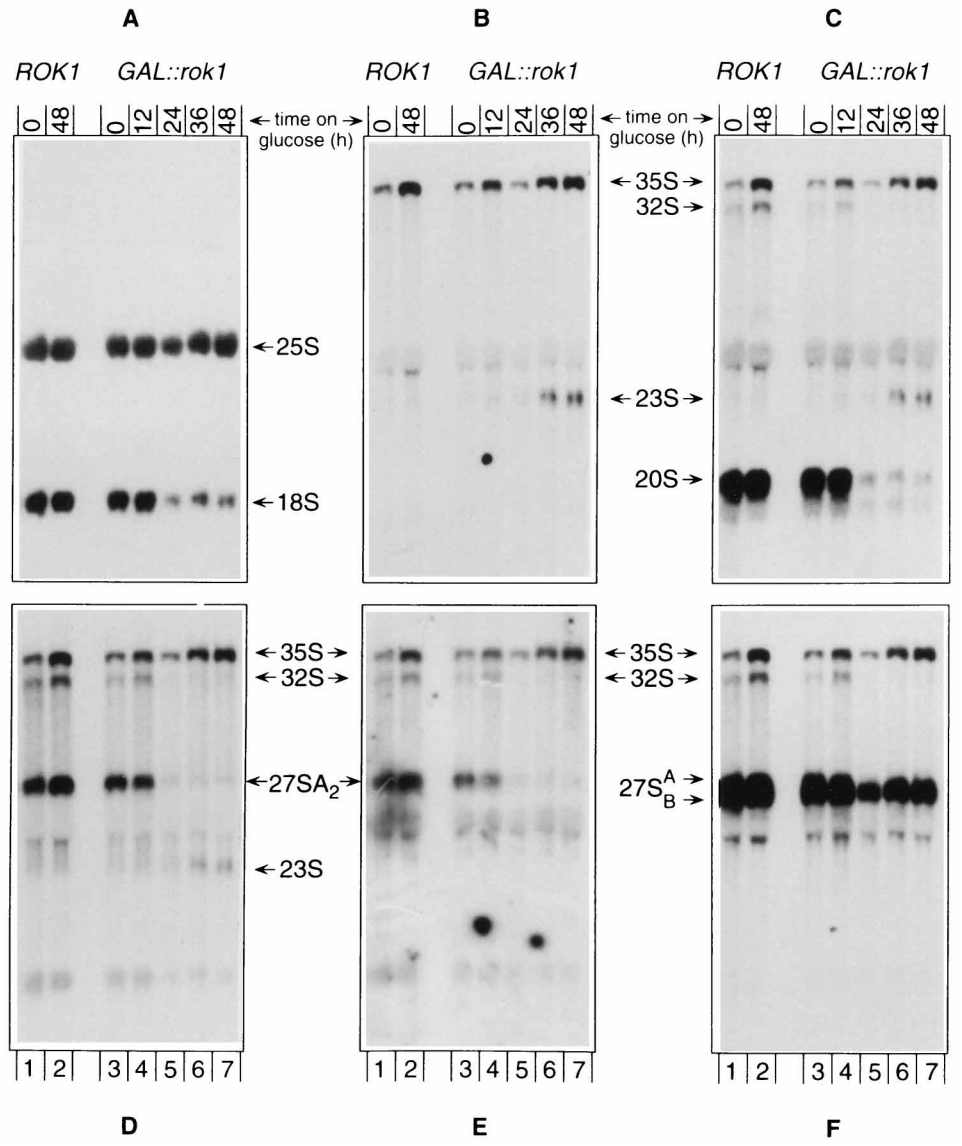

FIG. 4. Effect of Rok1p depletion on pre-rRNA processing. RNA was extracted from the *GAL::rok1* strain (YJV172) at t = 0, 12, 24, 36, and 48 h after transfer to glucose (lanes 3 to 7) and analyzed by Northern hybridization with oligonucleotides complementary to different regions of the pre-rRNA operon (see Fig. 1A for their location). As a control, RNA prepared from the *ROK1* strain (YJV156) at 0 and 48 h after transfer to glucose was used (lanes 1 and 2). The panels represent consecutive hybridizations of the same filter with the different probes. (A) Oligonucleotides 2 and 3, complementary to sites within the mature 18S and 25S rRNA sequences, respectively. (B) Oligonucleotide 1 in the 5′ ETS. (C) Oligonucleotide 4 in ITS1 upstream of site A_2. (D) Oligonucleotide 5 in ITS1 between sites A_2 and A_3. (E) Oligonucleotide 6 in ITS1 downstream of site A_3. (F) Oligonucleotide 7 in ITS2. The positions of the different pre-rRNAs are indicated by arrows.

severely reduced (Fig. 4A, compare lanes 1 to 4 and lanes 5 to 7). These data show that Rok1p is required for accumulation of 18S rRNA but not of 25S rRNA.

Rok1p is required for processing at A_0, A_1, and A_2. The effects of depletion of Rok1p on processing of the pre-rRNAs were analyzed by Northern hybridization with probes complementary to the transcribed spacer regions. The yeast pre-rRNA processing pathway is shown in Fig. 1, together with the locations of the oligonucleotide probes used to detect the different pre-rRNA species. Figure 4B to F present hybridizations of the filter shown in Fig. 4A with probes complementary to the 5′ ETS (Fig. 4B), ITS1 (Fig. 4C to E), and ITS2 (Fig. 4F).

Depletion of Rok1p results in a strong reduction in the levels of the pre-rRNA species 32S (Fig. 4B to F), 20S (Fig. 4C) and $27SA_2$ (Fig. 4D) following growth for 24 h in glucose medium. These pre-rRNA species are the products of cleavages at sites A_1 and A_2 (Fig. 1). The levels of the 27SB pre-rRNAs (Fig. 4F) are not affected, indicating that the major subsequent processing reaction, cleavage at site A_3, is not inhibited. A slightly increased accumulation of the 35S primary transcript is also observed (Fig. 4B to F), suggesting that the early cleavage at site A_0 in the 5′ ETS is delayed. Furthermore, an aberrant pre-rRNA species, designated 23S RNA, accumulates in the Rok1p-depleted strain. The 23S RNA is detected with probes in the 5′ ETS (Fig. 4B) and in ITS1 up to, but not beyond, site A_3 (compare Fig. 4C and D with Fig. 4E). It is therefore predicted to extend from the 5′ end of the 35S primary transcript to site A_3. This is the expected product of direct processing of the 35S pre-rRNA at site A_3 within ITS1

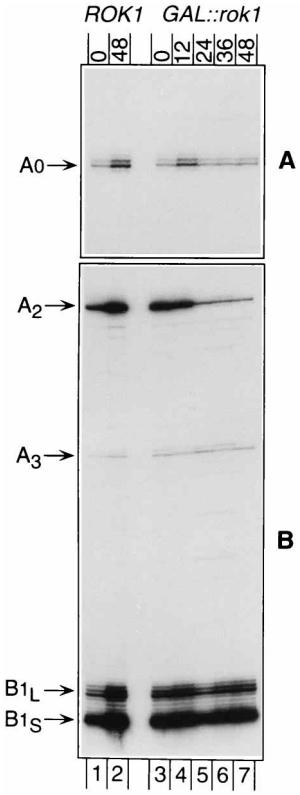

FIG. 5. Primer extension analysis of pre-rRNA from a Rok1p-depleted strain. The samples and lane order are as in Fig. 4. (A) Primer extension with oligonucleotide 2, priming within the mature 18S rRNA region. (B) Primer extension from oligonucleotide 7 within ITS2. The positions of primer extension stops corresponding to the different pre-rRNA cleavage sites are indicated.

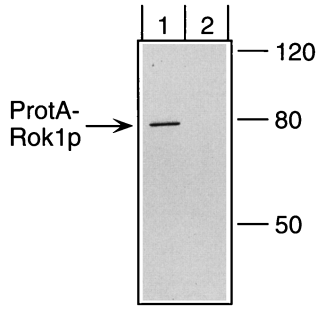

FIG. 6. Western blotting of ProtA-Rok1p. Whole-cell lysates were prepared from strains expressing Rok1p (YJV174 [lane 2]) or ProtA-Rok1p (YJV175 [lane 1]) and analyzed by Western blotting with rabbit peroxidase anti-peroxidase complex and an enhanced chemiluminescence detection kit. The positions of molecular mass markers (in kilodaltons) are indicated on the right, and the position of the ProtA-Rok1p protein is indicated on the left.

in the absence of cleavage at sites A_0, A_1, and A_2. Northern analysis of low-molecular-weight RNA species showed that the steady-state levels of the mature 5.8S rRNA species and of the 7S pre-rRNA were unaltered during depletion of Rok1p, indicating that processing in ITS2 is not affected (data not shown, but see Fig. 5B below).

Northern hybridization does not readily detect the 33S or $27SA_3$ pre-rRNAs and does not distinguish between the $27SB_L$ and $27SB_S$ precursors. These species were therefore analyzed by primer extension (Fig. 5). The level of the 33S pre-rRNA, shown by the primer extension stop at site A_0, is not clearly altered during Rok1p depletion (Fig. 5A). However, as described above, the appearance of the 23S RNA shows that A_0 cleavage is at least delayed in the Rok1p-depleted strain. The levels of the $27SA_3$, $27SB_L$, and $27SB_S$ pre-rRNAs, shown by the primer extension stops at sites A_3, $B1_L$, and $B1_S$, respectively, are also unaltered during Rok1p depletion (Fig. 5B). Consistent with the results of Northern hybridization, the level of $27SA_2$, shown by the primer extension stop at site A_2, is strongly reduced 24 h after transfer to glucose medium (Fig. 5B). Processing at sites A_0, A_1, A_2, A_3, $B1_L$, and $B1_S$ is correct at the nucleotide level in the Rok1p-depleted strain (Fig. 5 and data not shown).

Upon depletion of Rok1p, splicing of the actin (*ACT1*) pre-mRNA is not detectably inhibited, as shown by Northern hybridization with the actin intron as a probe (data not shown), indicating that Rok1p is not required for pre-mRNA splicing. In addition, several snoRNAs tested, U3, U14, U24, snR10, and snR30, accumulate to normal levels in the absence of Rok1p (data not shown).

Taken together, the results indicate that depletion of Rok1p leads to a specific inhibition of processing at the sites required for synthesis of the 18S rRNA, A_0, A_1 and A_2. Subsequent processing reactions in ITS1 and ITS2 which lead to synthesis of the 5.8S and 25S rRNAs do not require Rok1p. This phenotype is similar to that observed following genetic depletion of several different snoRNA species (64), but Rok1p is not required for accumulation of these snoRNAs.

Rok1p is localized predominantly in the nucleolus. To localize the Rok1p protein within the cell, an epitope-tagged fusion protein was constructed. An *Nco*I fragment containing two IgG-binding sites of *S. aureus* protein A was inserted in the *Nco*I site at the ATG start of the *ROK1* gene and cloned into the episomal vector pRS314 (CEN-TRP1), yielding pTRP1-ProtA::rok1. As a control, a plasmid containing the nontagged gene, pTRP1-ROK1, was used. Both plasmids were transformed into the *GAL::rok1* strain, YJV172, and tested for their ability to support growth on glucose medium. The growth rates of cells expressing either the *ROK1* gene or the *ProtA::rok1* gene were identical, demonstrating that ProtA-Rok1p is fully functional (data not shown). Western analysis with peroxidase-coupled rabbit IgG detected a single protein with an estimated molecular mass of 75 kDa in a whole-cell lysate from the *ProtA::rok1* strain (YJV175) but not from the *ROK1* strain (YJV174) (Fig. 6).

ProtA-Rok1p was immunoprecipitated from cell lysates with IgG-agarose beads, and bound proteins and RNAs were recovered (see Materials and Methods). Western blotting confirmed that ProtA-Rok1p was effectively precipitated although never with 100% efficiency (data not shown). Northern hybridization did not reveal detectable coprecipitation of the snoRNAs snR10, snR30, U3, or U14 (data not shown). Total coprecipitated RNAs were 3′ labeled with [5′-^{32}P]pCp and RNA ligase. No RNA was clearly enriched in the immunoprecipitate (data not shown). While masking of the ProtA epitope in the snoRNPs remains a formal possibility, it is probable that Rok1p is not stably associated with the snoRNPs.

Indirect immunofluorescence was performed with the strains expressing either ProtA-Rok1p or Rok1p following growth in glucose medium, by using a rabbit anti-protein A antibody. As a control, Nop1p was decorated with mouse monoclonal antibody MAb66 (3). To localize the nucleus, DNA was stained with DAPI (Fig. 7, right panels). With anti-Nop1p, both strains show the typical crescent-shaped staining

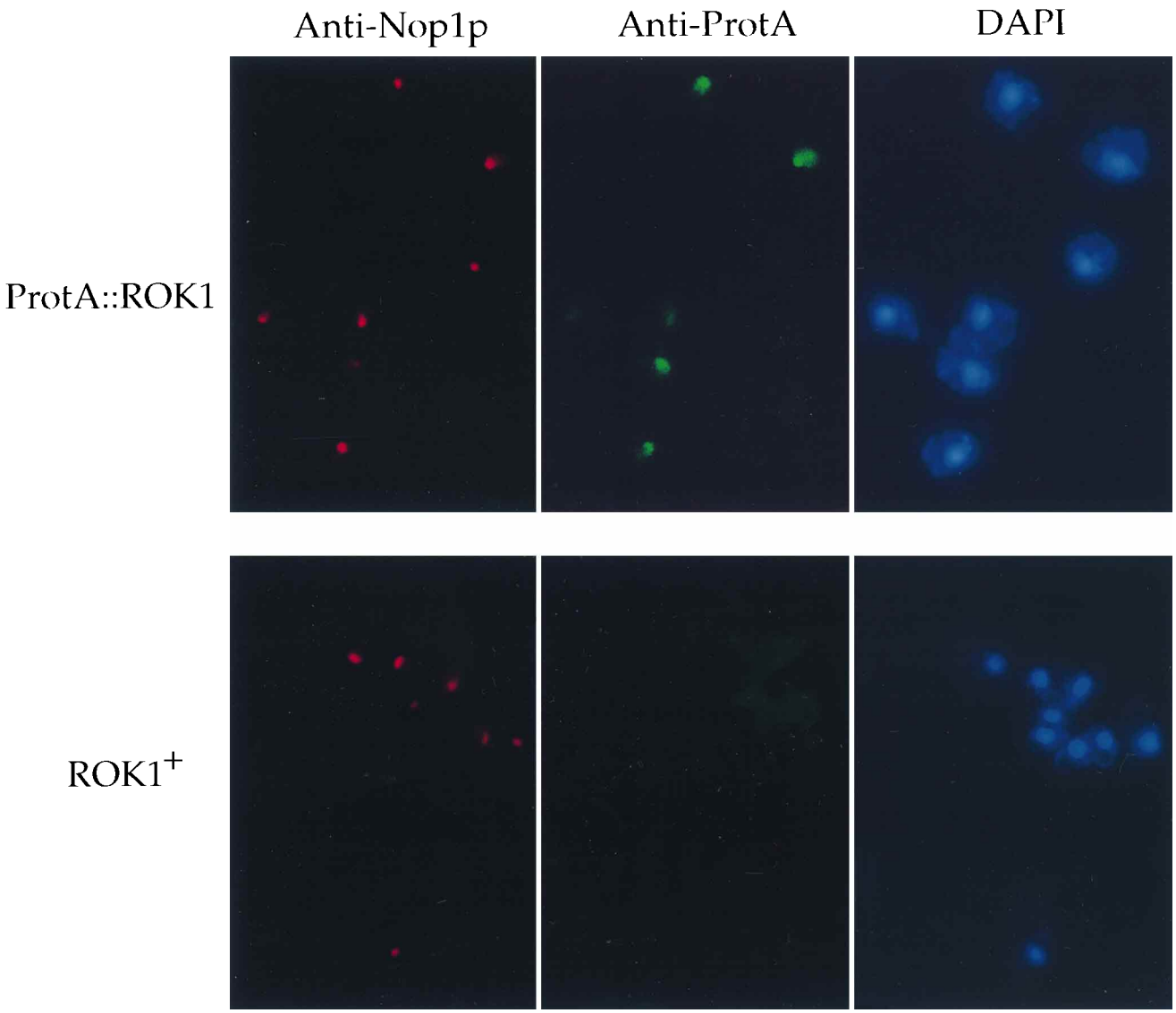

FIG. 7. Immunolocalization of ProtA-Rok1p. Indirect immunofluorescence was performed with cells expressing ProtA-Rok1p (YJV175 [upper panels]) and Rok1p (YJV174 [lower panels]). Nop1p was detected by mouse monoclonal antibody MAb66, followed by a goat anti-mouse antibody coupled to Texas red (left panels). ProtA-Rok1p was detected with a rabbit anti-protein A antibody and a goat anti-rabbit antibody coupled to FITC (middle panels). In addition, chromatin was stained with DAPI (right panels).

characteristic of nucleolar proteins (Fig. 7, left panels). With the anti-ProtA antibody, the *ROK1* strain shows only a very low background staining whereas the *ProtA::rok1* strain exhibits a nuclear signal (Fig. 7, middle panels) with nucleolar enrichment. We did not detect clear cytoplasmic staining with anti-ProtA in the *ProtA::rok1* cells. The predominant localization of ProtA-Rok1p in the nucleolus is in agreement with the prominent role of Rok1p in pre-rRNA processing.

DISCUSSION

We have performed screens for synthetic lethality with a deletion of the nonessential snoRNA, snR10, and with a mutant allele of the gene encoding the snoRNP protein, Gar1p. Both screens identified the same gene, *ROK1*, that encodes a putative, ATP-dependent RNA helicase of the DEAD-box protein family. Analysis of the effects of Rok1p depletion showed that, like snR10 and Gar1p, the protein functions in the synthesis of 18S rRNA. In the absence of Rok1p, the cleavages at A_0, A_1 and A_2 are inhibited and the products of these processing steps, the 32S, $27SA_2$ and 20S pre-rRNAs, are lost (Fig. 4). Direct cleavage of the 35S pre-rRNA at site A_3 within ITS1 generates the aberrant 23S pre-rRNA as the 5′-terminal product. This intermediate is not further processed to mature 18S rRNA and is rapidly degraded. The 3′-terminal product, $27SA_3$ pre-rRNA, is a normal processing intermediate and is converted to the mature 5.8S and 25S rRNAs in the mutant strain. This phenotype is similar to that observed following genetic depletion of components of the snR10, snR30, U3, and U14 snoRNPs (21, 28, 30, 38, 44, 61). In strains depleted of Gar1p or the U14, snR10, or snR30 snoRNAs, processing at site A_0 appears to be less inhibited than is processing at sites A_1 or A_2 (5, 64), and this is also the case for Rok1p. The accumulation of the 35S pre-rRNA and the aberrant 23S RNA in all of these mutants indicates that cleavage at

A_0 is, however, kinetically delayed (further discussed in references 34 and 64).

Processing at A_0, A_1, and A_2 has been suggested to take place in a large complex containing the U3, U14, snR10, and snR30 snoRNAs (45). Gar1p is a component of the snR10 and snR30 snoRNPs (4, 21) and would therefore also participate in the putative complex. The similarities in the phenotypes observed upon depletion of Gar1p and snR30 suggest that inactivation of the snR30 snoRNP gives rise to the observed phenotypes in both cases (21, 44). Loss of the snR10 snoRNP gives a similar but weaker phenotype (59), and the effects of Gar1p depletion on its activity cannot therefore be readily assessed. Since mutations in *ROK1* are *sl* with mutations in either *SNR10* or *GAR1*, it is possible that *rok1* mutations are *sl* with the loss of function of the snR10 snoRNP. This is supported by the fact that the *rok1-2* mutation, identified in the *sl* screen with *gar1-10*, is also *sl* with deletion of *SNR10* in strain YJV167. It is also interesting that the *gar1-10* allele codes for a protein that is truncated at position 158, thereby deleting the glycine-arginine-rich (GAR) domain of Gar1p (see also references 20 and 21). In the nucleolar protein nucleolin, this structure contains ATP-simulated RNA-unfolding activity similar to that exhibited by some DEAD-box proteins (17, 63). The synthetic lethality between the *rok1-2* and *gar1-10* alleles might therefore be explained by cumulative defects in RNA unwinding reactions taking place during pre-rRNA processing and ribosome assembly.

The U3 and U14 snoRNAs bind to the pre-rRNA at sites within the 5′ ETS and the 18S rRNA region, respectively, through extended base pairing (5, 7, 39) which appears to be too long for ready dissociation in the absence of a helicase activity. In contrast, snR10 and snR30 lack sequences with extended complementarity to the pre-rRNA, but it remains possible that a helicase activity associated with Rok1p is required for their association with, or dissociation from, the pre-rRNA. In comparison, the involvement of DEAD/H-box proteins in pre-mRNA splicing has been well established, although it appears that most of these proteins interact only transiently with the spliceosome (reviewed in reference 15). For none of these proteins has it been demonstrated that they actually exhibit an RNA helicase activity, but the majority have been shown to possess RNA-stimulated ATPase activity in vitro. Recently, the latter activity has been demonstrated for a human protein which appears to be intrinsic to the U5 snRNP (35). The fact that we have been unable to detect coimmunoprecipitation of any snoRNA (or other RNA species) with ProtA-Rok1p therefore does not exclude the possibility that Rok1p physically interacts with one or more of the snoRNPs required for 18S rRNA synthesis. Rok1p is not simply required for the synthesis of the snoRNAs, since the accumulation of all species tested, including snR10 and snR30, was unaffected by Rok1p depletion.

Apart from pre-rRNA processing, ribosome biogenesis comprises rRNA modification reactions and assembly with the approximately 80 ribosomal proteins. Extensive structural rearrangements are expected to occur during all of these reactions, which are likely to require *trans*-acting factors. Strains lacking snR10 are impaired in growth, but the physical basis of this is unclear (59, 60). Pre-rRNA processing is clearly delayed in the mutant, but overall synthesis of the mature 18S rRNA is not reduced, and no difference in the accumulation of 18S and 25S rRNA is observed. Moreover, the growth of *snr10* mutant strains is partially cold sensitive, whereas the pre-rRNA-processing defect is entirely nonconditional. Together, these observations suggest that the impaired growth of *snr10* mutant strains may be due to a defect in ribosome assembly or rRNA modification rather than to the observed pre-rRNA-processing defect. Many mutants of *E. coli* that are defective in ribosome assembly are cold sensitive (12, 14, 25), and the cold sensitive phenotypes associated with the *snr10* and *rok1-2* mutations would therefore be consistent with a defect in ribosomal assembly. An RNA helicase activity associated with Rok1p might also be required during ribosome assembly or modification, with the impaired pre-rRNA processing appearing as a consequence of this.

It is notable that several other putative RNA helicases have been shown to be involved in ribosome assembly in both *E. coli* and yeast. The bacterial SrmB and DeaD proteins can suppress mutations which cause defective assembly of the large and small ribosomal subunit, respectively (48, 62), while the ATPase activity of DbpA is specifically stimulated by a fragment of the bacterial 23S rRNA containing the peptidyltransferase center (16, 47). In yeast, the putative helicases Spb4p (52) and Drs1p (50) are required for assembly of the 60S ribosomal subunit and synthesis of the 25S rRNA, while Rrp3p is required for the synthesis of yeast 18S rRNA (49). Genetic depletion of Rrp3p also inhibits pre-rRNA processing at sites A_0, A_1, and A_2, but although depletion of Rok1p or Rrp3p gives a similar phenotype, it is clear from the genetic results that they have distinct functions. Thus, yeast ribosome synthesis requires at least four DEAD-box proteins, each with its unique function, and it is likely that more members of this protein class will be identified.

ACKNOWLEDGMENTS

We thank John P. Aris (University of Florida, Gainesville, Fla.) for the gift of the anti-Nop1p antibody. We gratefully acknowledge the experimental assistance of Christophe Normand (LBME) and Hildegard Tekotte (EMBL). We thank Yves Henry, Dick Raué, and Rienk Jeeninga for critical reading of the manuscript.

J.V. was the recipient of an HCM fellowship from the European Union. C.B.A was the recipient of a fellowship from l'Association pour la Recherche contre le Cancer (ARC). This work was supported by the Ministère de l'Enseignement Supérieur et de la Recherche (ACC1), l'ARC, Région Midi-Pyrénées, Ligue Nationale contre le Cancer, CNRS, and the Université Paul Sabatier.

REFERENCES

1. **Abou Elela, S., H. Igel, and M. Ares, Jr.** 1996. RNase III cleaves eukaryotic preribosomal RNA at a U3 snoRNP-dependent site. Cell **85:**115–124.
2. **Amberg, D. C., A. L. Goldstein, and C. N. Cole.** 1992. Isolation and characterization of RAT1: an essential gene of *Saccharomyces cerevisiae* required for the efficient nucleocytoplasmic trafficking of mRNA. Genes Dev. **6:**1173–1189.
3. **Aris, P., and G. Blobel.** 1988. Identification and characterization of a yeast nucleolar protein that is similar to a rat liver nucleolar protein. J. Cell Biol. **107:**17–31.
4. **Balakin, A. G., L. Smith, and M. J. Fournier.** 1996. The RNA world of the nucleolus: two major families of small RNAs defined by different box elements with related functions. Cell **86:**823–834.
5. **Beltrame, M., Y. Henry, and D. Tollervey.** 1994. Mutational analysis of an essential binding site for the U3 snoRNA in the 5′ external transcribed spacer of yeast pre-rRNA. Nucleic Acids Res. **22:**5139–5147.
6. **Beltrame, M., and D. Tollervey.** 1992. Identification and functional analysis of two U3 binding sites on yeast pre-ribosomal RNA. EMBO J. **11:**1531–1542.
7. **Beltrame, M., and D. Tollervey.** 1995. Base pairing between U3 and the pre-ribosomal RNA is required for 18S rRNA synthesis. EMBO J. **14:**4350–4356.
8. **Berben, G., J. Dumont, V. Gilliquet, P.-A. Bolle, and F. Hilger.** 1991. The YDp plasmids: a uniform set of vectors bearing versatile disruption cassettes for *Saccharomyces cerevisiae*. Yeast **7:**475–477.
9. **Bergès, T., E. Petfalski, D. Tollervey, and E. C. Hurt.** 1994. Synthetic lethality with fibrillarin identifies NOP77p, a nucleolar protein required for pre-rRNA processing and modification. EMBO J. **13:**3136–3148.
10. **Cadwell, R. C., and G. F. Joyce.** 1992. Randomization of genes by PCR mutagenesis. PCR Methods Appl. **2:**28–33.
11. **Chu, S., R. H. Archer, J. M. Zengel, and L. Lindahl.** 1994. The RNA of RNase MRP is required for normal processing of ribosomal RNA. Proc. Natl. Acad. Sci. USA **91:**659–663.

12. **Dammel, C. S., and H. F. Noller.** 1993. A cold-sensitive mutation in 16S rRNA provides evidence for helical switching in ribosome assembly. Genes Dev. **7:**660–670.
13. **Eichler, D. C., and N. Craig.** 1994. Processing of eukaryotic ribosomal RNA. Prog. Nucleic Acid Res. Mol. Biol. **49:**197–239.
14. **Feunteun, J., R. Monier, C. Vola, and R. Rosset.** 1974. Ribosomal assembly defective mutants of *Escherichia coli*. Nucleic Acids Res. **1:**149–169.
15. **Fuller-Pace, F. V.** 1994. RNA helicases: modulators of RNA structure. Trends Cell Biol. **4:**271–274.
16. **Fuller-Pace, F. V., S. M. Nicol, A. D. Reid, and D. P. Lane.** 1993. DbpA: a DEAD box protein specifically activated by 23S rRNA. EMBO J. **12:**3619–3626.
17. **Ghisolfi, L., G. Joseph, F. Amalric, and M. Erard.** 1992. The glycine-rich domain of nucleolin has an unusual supersecondary structure responsible for its RNA-helix-destabilizing properties. J. Biol. Chem. **267:**2955–2959.
18. **Gietz, D., A. St. Jean, R. A. Woods, and R. H. Schiestl.** 1992. Improved method for high efficiency transformation of intact yeast cells. Nucleic Acids Res. **20:**1425.
19. **Gietz, R. D., and A. Sugino.** 1988. New yeast-*Escherichia coli* shuttle vectors constructed with in vitro mutagenized yeast genes lacking six-base pair restriction sites. Gene **74:**527–534.
20. **Girard, J. P., C. Bagni, M. Caizergues-Ferrer, F. Amalric, and B. Lapeyre.** 1994. Identification of a segment of the small nucleolar ribonucleoprotein-associated protein GAR1 that is sufficient for nucleolar accumulation. J. Biol. Chem. **269:**18499–18506.
21. **Girard, J. P., H. Lehtonen, M. Caizergues-Ferrer, F. Amalric, D. Tollervey, and B. Lapeyre.** 1992. GAR1 is an essential small nucleolar RNP protein required for pre-rRNA processing in yeast. EMBO J. **11:**673–682.
22. **Grandi, P., V. Doyl, and E. C. Hurt.** 1993. Purification of NSP1 reveals complex formation with 'GLFG' nucleporins and a novel nuclear pore protein NIC96. EMBO J. **12:**3061–3071.
23. **Guarente, L., R. R. Yocum, and P. Gifford.** 1982. A *GAL10-CYC1* hybrid yeast promoter identifies the *GAL4* regulatory region as an upstream site. Proc. Natl. Acad. Sci. USA **79:**7410–7414.
24. **Gururajan, R., L. Mathews, F. J. Longo, and D. L. Weeks.** 1994. An3 mRNA encodes an RNA helicase that colocalizes with nucleoli in *Xenopus* oocytes in a stage-specific manner. Proc. Natl. Acad. Sci. USA **91:**2056–2060.
25. **Guthrie, C., H. Nashimoto, and M. Nomura.** 1969. Structure and function of *E. coli* ribosomes. VIII. Cold-sensitive mutants defective in ribosome assembly. Proc. Natl. Acad. Sci. USA **63:**384–391.
26. **Henry, Y., H. Wood, J. P. Morrissey, E. Petfalski, S. Kearsey, and D. Tollervey.** 1994. The 5′ end of yeast 5.8S rRNA is generated by exonucleases from an upstream cleavage site. EMBO J. **13:**2452–2463.
27. **Hsu, C. L., and A. Stevens.** 1993. Yeast cells lacking 5′ 3 3′ exoribonuclease 1 contain mRNA species that are poly(A) deficient and partially lack the 5′ cap structure. Mol. Cell. Biol. **13:**4826–4835.
28. **Hughes, J. M. X., and M. J. Ares.** 1991. Depletion of U3 small nucleolar RNA inhibits cleavage in the 5′ external transcribed spacer of yeast preribosomal RNA and impairs formation of 18S ribosomal RNA. EMBO J. **10:**4231–4239.
29. **Interthal, H., C. Bellocq, J. Bähler, V. I. Bashkirov, S. Edelstein, and W.-D. Heyer.** 1995. A role of Sep1 (=Kem1, Xrn1) as a microtubule-associated protein in *Saccharomyces cerevisiae*. EMBO J. **14:**1057–1066.
30. **Jansen, R., D. Tollervey, and E. C. Hurt.** 1993. A U3 snoRNP protein with homology to splicing factor PRP4 and Gβ domains is required for ribosomal RNA processing. EMBO J. **12:**2549–2558.
31. **Kearsey, S., and D. Kipling.** 1991. Recombination and RNA processing: a common strand? Trends Cell Biol. **1:**110–112.
32. **Koshland, D., J. C. Kent, and L. H. Hartwell.** 1985. Genetic analysis of the mitotic transmission of minichromosomes. Cell **40:**393–403.
33. **Kranz, J. E., and C. Holm.** 1990. Cloning by function: an alternative approach for identifying yeast homologs of genes from other organisms. Proc. Natl. Acad. Sci. USA **87:**6629–6633.
34. **Lafontaine, D., and D. Tollervey.** 1995. *trans*-acting factors in yeast pre-rRNA and pre-snoRNA processing. Biochem. Cell Biol. **73:**803–812.
35. **Laggerbauer, B., J. Lauber, and R. Lührmann.** 1996. Identification of an RNA-dependent ATPase activity in mammalian U5 snRNPs. Nucleic Acids Res. **24:**868–875.
36. **Larimer, F. W., C. L. Hsu, M. K. Maupin, and A. Stevens.** 1992. Characterization of the *XRN1* gene encoding a 5′ 3 3′ exoribonuclease: sequence data and analysis of disparate protein and mRNA levels of gene-disrupted yeast cells. Gene **120:**51–57.
37. **Larimer, F. W., and A. Stevens.** 1990. Disruption of the gene *XRN1*, coding for a 5′ 3 3′ exoribonuclease, restricts yeast cell growth. Gene **95:**85–90.
38. **Li, H. V., J. Zagorski, and M. J. Fournier.** 1990. Depletion of U14 small nuclear RNA (snR128) disrupts production of 18S rRNA in *Saccharomyces cerevisiae*. Mol. Cell. Biol. **10:**1145–1152.
39. **Liang, W.-Q., and M. J. Fournier.** 1995. U14 base pairs with 18S rRNA: a novel snoRNA interaction required for rRNA processing. Genes Dev. **9:**2433–2443.
40. **Lygerou, Z., C. Allmang, D. Tollervey, and B. Séraphin.** 1996. Accurate processing of a eukaryotic precursor ribosomal RNA by ribonuclease MRP *in vitro*. Science **272:**268–270.
41. **Lygerou, Z., P. Mitchell, E. Petfalski, B. Séraphin, and D. Tollervey.** 1994. The *POP1* gene encodes a protein component common to the RNase MRP and RNase P ribonucleoproteins. Genes Dev. **8:**1423–1433.
42. **Maxwell, E. S., and M. J. Fournier.** 1995. The small nucleolar RNAs. Annu. Rev. Biochem. **35:**897–934.
43. **Mélèse, T., and Z. Xue.** 1995. The nucleolus: an organelle formed by the act of building a ribosome. Curr. Opin. Cell Biol. **7:**319–324.
44. **Morrissey, J. P., and D. Tollervey.** 1993. Yeast snR30 is a small nucleolar RNA required for 18S rRNA synthesis. Mol. Cell. Biol. **13:**2469–2477.
45. **Morrissey, J. P., and D. Tollervey.** 1995. Birth of the snoRNPs—the evolution of RNase MRP and the eukaryotic pre-rRNA processing system. Trends Biochem. Sci. **20:**78–82.
46. **Muhlrad, D., C. J. Decker, and R. Parker.** 1994. Deadenylation of the unstable mRNA encoded by the yeast *MFA2* gene leads to decapping followed by 5′ 3 3′ digestion of the transcript. Genes Dev. **8:**855–866.
47. **Nicol, S. M., and F. V. Fuller-Pace.** 1995. The "DEAD box" protein DbpA interacts specifically with the peptidyltransferase center in 23S rRNA. Proc. Natl. Acad. Sci. USA **92:**11681–11685.
48. **Nishi, K., F. Morel-Deville, J. W. Hershey, T. Leighton, and J. Schnier.** 1988. An eIF-4A-like protein is a suppressor of an *Escherichia coli* mutant defective in 50S ribosomal subunit assembly. Nature **336:**496–498.
49. **O'Day, C. L., F. Chavanikamannil, and J. Abelson.** 1996. 18S rRNA processing requires the RNA-helicase-like protein Rrp3. Nucleic Acids Res. **24:**3201–3207.
50. **Ripmaster, T. L., G. P. Vaughn, and J. L. Woolford, Jr.** 1992. A putative ATP-dependent RNA helicase involved in *Saccharomyces cerevisiae* ribosome assembly. Proc. Natl. Acad. Sci. USA **89:**11131–11135.
51. **Rothstein, R.** 1990. Targeting, disruption, replacement and allele rescue: integrative DNA transformation in yeast. Methods Enzymol. **194:**281–301.
52. **Sachs, A. B., and R. W. Davis.** 1990. Translation initiation and ribosomal biogenesis: involvement of a putative rRNA helicase and RPL46. Science **247:**1077–1079.
53. **Sambrook, J., E. F. Fritsch, and T. Maniatis.** 1989. Molecular cloning: a laboratory manual, 2nd ed. Cold Spring Harbor Laboratory Press, Cold Spring Harbor, N.Y.
54. **Schmid, S. R., and P. Linder.** 1992. D-E-A-D protein family of putative RNA helicases. Mol. Microbiol. **6:**283–292.
55. **Schmitt, M. E., and D. A. Clayton.** 1993. Nuclear RNase MRP is required for correct processing of pre-5.8S rRNA in *Saccharomyces cerevisiae*. Mol. Cell. Biol. **13:**7935–7941.
56. **Song, Y., S. Kim, and J. Kim.** 1995. *ROK1*, a high-copy number plasmid suppressor of *KEM1*, encodes a putative ATP-dependent RNA helicase in *Saccharomyces cerevisiae*. Gene **166:**151–154.
57. **Stevens, A., C. L. Hsu, K. R. Isham, and F. W. Larimer.** 1991. Fragments of the internal transcribed spacer 1 of pre-rRNA accumulate in *Saccharomyces cerevisiae* lacking 5′ 3 3′ exoribonuclease 1. J. Bacteriol. **173:**7024–7028.
58. **Stevens, A., and T. L. Poole.** 1995. 5′-Exonuclease-2 of *Saccharomyces cerevisiae*. J. Biol. Chem. **270:**16063–16069.
59. **Tollervey, D.** 1987. A yeast small nuclear RNA is required for normal processing of pre-ribosomal RNA. EMBO J. **6:**4169–4175.
60. **Tollervey, D., and C. Guthrie.** 1985. Deletion of a yeast small nuclear RNA gene impairs growth. EMBO J. **4:**3873–3878.
61. **Tollervey, D., H. Lehtonen, M. Carmo-Fonseca, and E. C. Hurt.** 1991. The small nucleolar RNP protein NOP1 (fibrillarin) is required for pre-rRNA processing in yeast. EMBO J. **10:**573–583.
62. **Toone, W. M., K. E. Rudd, and J. D. Friesen.** 1991. *deaD*, a new *Escherichia coli* gene encoding a presumed ATP-dependent RNA helicase, can suppress a mutation in *rpsB*, the gene encoding ribosomal protein S2. J. Bacteriol. **173:**3291–3302.
63. **Tuteja, N., N. W. Huang, D. Skopac, R. Tuteja, S. Hrvatic, J. Zhang, S. Pongor, G. Joseph, C. Faucher, F. Amalric, and A. Falaschi.** 1995. Human DNA helicase IV is nucleolin, an RNA helicase modulated by phosphorylation. Gene **160:**143–148.
64. **Venema, J., and D. Tollervey.** 1995. Processing of pre-ribosomal RNA in *Saccharomyces cerevisiae*. Yeast **11:**1629–1650.
65. **Venema, J., and D. Tollervey.** 1996. *RRP5* is required for formation of both 18S and 5.8S rRNA in yeast. EMBO J. **15:**5701–5714.